JACS
JOURNAL OF THE AMERICAN CHEMICAL SOCIETY
Article
pubs.acs.org/JACS

Electrochemistry of a Single Attoliter Emulsion Droplet in Collisions

Byung-Kwon Kim, Jiyeon Kim, and Allen J. Bard*

Center for Electrochemistry, Department of Chemistry and Biochemistry, The University of Texas at Austin, Austin, Texas 78712, United States

ABSTRACT: We report here the electrochemistry of emulsion droplets by observing single emulsion droplet collisions with selective electrochemical reduction on an ultramicroelectrode (UME). With appropriately applied potentials at an UME, we can observe the electrochemical effects of single collision signals from the complete electrolysis of single emulsion droplets, or selective electrolysis of redox species in single emulsion droplets. This was observed with nitrobenzene (NB), 7,7,8,8-tetracyanoquinodimethane (TCNQ), and ionic liquid. The NB, TCNQ, and ionic liquid act as emulsion material, redox specie, and emulsifier (and electrolyte), respectively. NB emulsions and NB (TCNQ) emulsions were made by ultrasonic processing. During the amperometric current−time (i−t) curve measurement with NB/water emulsion at −0.65 V, reduction of NB emulsion droplets was measured. In the case of less negative potentials, e.g., at −0.45 V with a NB (TCNQ) emulsion, selective reduction of TCNQ in NB droplet was measured. Spike-like responses from electrolysis of NB or TCNQ in each experiment were observed. From these single-particle collision results of NB and NB (TCNQ) emulsions, the collision frequency, size distribution, i−t decay behavior of emulsion droplets, and possible mechanisms are discussed.

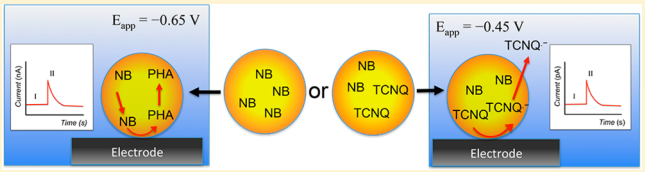

1. INTRODUCTION

There has been considerable activity in the field of single-particle collisions for over a decade, since it allows one to obtain important information on single-particle properties, e.g., catalytic activity, size, and lifetime, that is not available in ensemble results.[1−9] So far, most single-particle collision experiments have been focused on "hard" particles such as metal nanoparticles (Pt, Au, Cu, Ag),[1−5] oxides (IrO_2, TiO_2),[6,7] and dielectrics (polystyrene, SiO_2).[8,9] Recently, we extended the single-particle collision research to "soft" (or "liquid") particles such as emulsions. Previously, we proposed two kinds of new methods to study single soft particle collisions in emulsions.[10] Briefly, we used oil emulsion droplets (e.g., toluene) containing hydrophobic redox molecules (e.g., ferrocene) and an ionic liquid, which can collide with an ultramicroelectrode (UME) in an aqueous continuous phase under an oxidation potential. Once the emulsion droplets collide, redox molecules inside the oil emulsion droplet start to be electrolyzed, and accordingly, a spike type of current increase is observed during the current−time (i−t) measurements. In this method, emulsion droplets act as a reactor of redox molecules; thus, we call this the emulsion droplet reactor (EDR) method. In another example, we used a high concentration of hydrophilic redox molecules (200 mM potassium ferrocyanide) in the aqueous continuous phase containing the same emulsion droplets, where the UME is biased at the potential for the oxidation of ferrocyanide. At the beginning of the amperometric i−t curve measurements, the steady-state current of electrolysis of hydrophilic potassium ferrocyanide is observed. When an emulsion droplet collides and sticks to the UME, the flux of redox molecules in the aqueous continuous phase to the UME is hindered by the presence of the emulsion droplet, leading to a decrease in the steady-state current. As a result, such a blocking by the droplet collision decreases the current in a staircase corresponding to each collision event. This is called emulsion droplet blocking (EDB). These EDR and EDB methods gave a collision signal from a single emulsion droplet, which enables one to gain information about the stochastic events such as droplet size distribution, collision frequency, and droplet contents. These suggested concepts can provide a better understanding for the collision of other types of single "soft" particles with an UME in previously published papers based on single liposome and vesicle detection methods.[11−16] Also, we discuss the ion transfer across the droplet interface between organic and water phase as reported by Scholz for his 2 μL droplet.[17]

In this paper, we report newly extended results from EDR studies. The EDR method is very useful in studies of very tiny reactors (attoliter or less),[18,19] collectors, and sensors; therefore, a deeper understanding of this EDR method is a prerequisite for its extensive application. In a previous paper, we showed the oxidation reaction of redox molecules occurring in a single emulsion droplet with ferrocene, an ionic liquid, and toluene.[10] Here, we further explore the reduction electrochemistry inside a single emulsion droplet containing 7,7,8,8-tetracyanoquinodimethane (TCNQ), an ionic liquid, and nitrobenzene (NB) (Figure 1A). TCNQ was chosen as a redox molecule in a single emulsion droplet, and NB serves as very tiny (attoliter) reactor. The ionic liquid was used as the emulsifier and the electrolyte. In this experiment, a spike type of transient current from the reduction of TCNQ was observed

Received: November 25, 2014
Published: January 23, 2015

DOI: 10.1021/ja512065n
J. Am. Chem. Soc. 2015, 137, 2343−2349

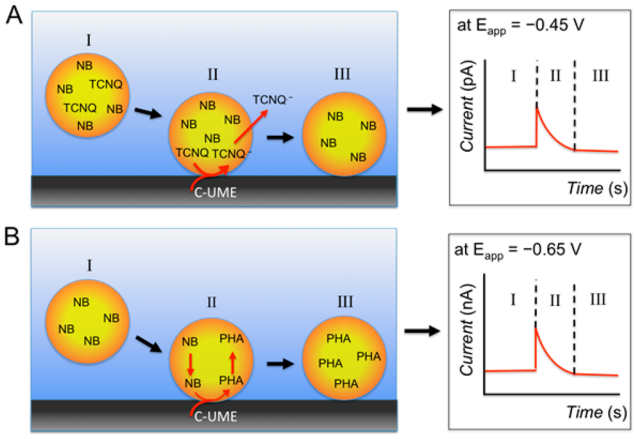

Figure 1. Schematic diagram of (A) selective electrochemical reduction of TCNQ in single NB (TCNQ) emulsion droplet, and (B) electrochemical reduction of single NB emulsion droplet at C-UME.

at the moment an emulsion collided with an UME. In addition, we investigate the electrochemistry of the reactor itself. Some redox-active organic molecules (e.g., NB) are hydrophobic enough to form an emulsion droplet and simultaneously behave as a redox mediator for an electrolysis reaction. Using these molecules, we could extend the electrochemistry occurring inside a droplet reactor to the reaction of a reactor itself as described in Figure 1B. In this regard, NB can be a good candidate. NB is only slightly soluble in water, while it is a good solvent for hydrophobic molecules, so that it easily forms an emulsion, and provides emulsion droplet reactors for other molecule's electrochemistry. Owing to the redox-active property, NB undergoes an electrochemical reduction reaction; thus, we can easily track it by the current. Since the entire droplet of NB is reducible, we can expect a large current signal due to the high concentration of NB (ca. 8.15 M) in the emulsion droplet. These newly proposed concepts and the experimental studies allow one to understand the droplet electrochemistry better and thereby uncover possible practical applications.

2. EXPERIMENTAL SECTION

2.1. Reagents and Materials. Nitrobenzene (NB, 99%+), 7,7,8,8-tetracyanoquinodimethane (TCNQ, 98%), trihexyltetradecylphosphonium bis(2,4,4-trimethylpentyl) phosphinate (IL-PP, >95.0%), ferrocenemethanol (97%), hexane (>95%), toluene (99.9%), isopropyl alcohol (IPA, >99.9%), and ethanol (99.9%) were obtained from Sigma or Aldrich. Sodium phosphate monobasic monohydrate (99.5% +), sodium phosphate dibasic anhydrous (99%), and potassium chloride (99%) were obtained from Fisher Scientific. All chemicals were used as received. Carbon fiber (diameter 10 μm) was obtained from Goodfellow (Devon, PA). Borosilicate capillary tubing (1.5 mm o.d. × 0.75 mm i.d.) was obtained from FHC Inc. (Bowdoin, ME). Millipore water (>18 MΩ·cm) was used in all experiments.

2.2. Instrumentation. The electrochemical experiments were performed using a CHI model 900B potentiostat (CH Instruments, Austin, TX) with a three-electrode cell placed in a faraday cage. A 0.5 mm diameter Pt was used as a counter electrode, and the reference electrode was Ag/AgCl (3 M NaCl). A Q500 ultrasonic processor (Qsonica, Newtown, CT) with a microtip probe was used to make the emulsions. Dynamic laser scattering (DLS) studies employed a Zetasizer Nano ZS (Malvern, Westborough, MA).

2.3. Preparation of Carbon Fiber Ultramicroelectrodes (C-UMEs). C-UME was prepared following the general procedure developed in our laboratory. Briefly, a 10 μm (diameter) carbon fiber was sealed in a borosilicate glass tubing (1.5 mm o.d. × 0.75 mm i.d.) after rinsing with hexane, toluene, IPA, ethanol, and water. The electrode was then polished with an alumina powder water suspension to a mirror finish. The surface area was checked with standard redox electrochemistry in ferrocenemethanol solution. Before every experiment, all electrodes were polished with alumina (0.05 μm) paste on microcloth pads (Buehler, Lake Bluff, IL) prior to use.

2.4. Preparation of NB (TCNQ) Emulsions and NB Emulsions. NB (TCNQ) emulsions were prepared by dissolving TCNQ (20 mM) and IL-PP (200 mM) in NB. The 0.1 mL mixture of NB was added to 5 mL of NB saturated water. The NB saturated water was used intentionally to maintain the size of NB emulsion droplet over the experimental time despite the low solubility in water (0.19 g NB/100 mL water at 20 °C). After that, the mixture solution was vigorously stirred for 30 s by vortex mixer. Consecutively, ultrasonic power (500 W, amplitude 40%) was applied using pulse mode (7 s on, 3 s off, 10 cycles repeated). The average diameter of created NB (TCNQ) emulsion droplets was 291 nm measured by DLS. The concentration of NB (TCNQ) emulsion droplets was approximately calculated from the total NB (TCNQ) volume (0.1 mL) divided by the average emulsion droplet volume (12.9 aL, assumed to be spherical with diameter 291 nm).

The NB emulsions were prepared as above without TCNQ. The average diameter of a NB droplet in the emulsion was approximately calculated from the total NB volume (0.1 mL) divided by the average emulsion droplet volume (5.96 aL, assumed to be spherical) gave a diameter 225 nm.

3. RESULTS AND DISCUSSION

3.1. Single Collision Events of NB (TCNQ) Emulsion Droplets. *3.1.1. Electrochemical Reduction of TCNQ in Bulk NB Solution with 200 mM IL-PP.* Cyclic voltammetry (CV) on a 10 μm C-UME was measured to demonstrate the electrochemical reduction of 20 mM TCNQ in bulk NB solution with 200 mM IL-PP for comparison with the same reaction within an emulsion droplet (Figure 2). The CV shows

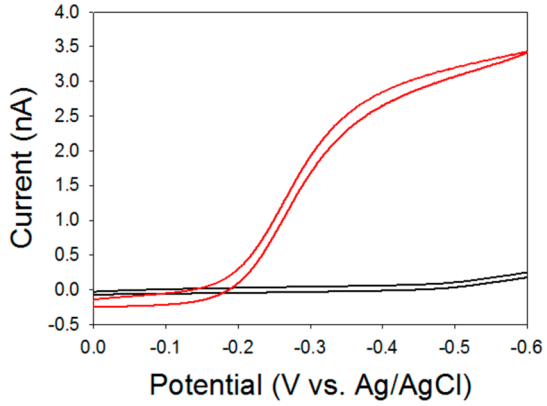

Figure 2. CVs of neat NB and 200 mM IL-PP with 20 mM TCNQ (red line) and without TCNQ (black line) at a scan rate of 50 mV s^{-1}.

a nearly retraceable sigmoidal wave of one electron TCNQ electrochemical reduction and is slightly distorted (red line in Figure 2). The reduction of TCNQ begins around −0.15 V (vs Ag/AgCl) and showed steady-state current around −0.4 V. The reduction of NB starts at −0.5 V (black line in Figure 2), so if we apply a potential around −0.4 to −0.5 V, we can selectively reduce TCNQ in a NB solution. The same NB composition was used to make the emulsion for reduction chemistry of a single emulsion droplet. Prepared NB (TCNQ) emulsions (dispersed phase) were introduced into a NB saturated water (continuous phase) for the collision experiments shown below.

DOI: 10.1021/ja512065n
J. Am. Chem. Soc. 2015, 137, 2343−2349

Here, we also used a NB saturated water as the electrochemical measurement medium to minimize the volume change of NB emulsion droplets during the full experimental time.

3.1.2. Collision Experiments of NB (TCNQ) Emulsion Droplets. Amperometric *i*−*t* curves were measured to monitor the collision of NB (TCNQ) droplets on a C-UME, resulting in the reduction of TCNQ to $TCNQ^{\bullet-}$ inside the NB emulsion droplets (Figure 3). As seen in Figure 3, a spike type of current

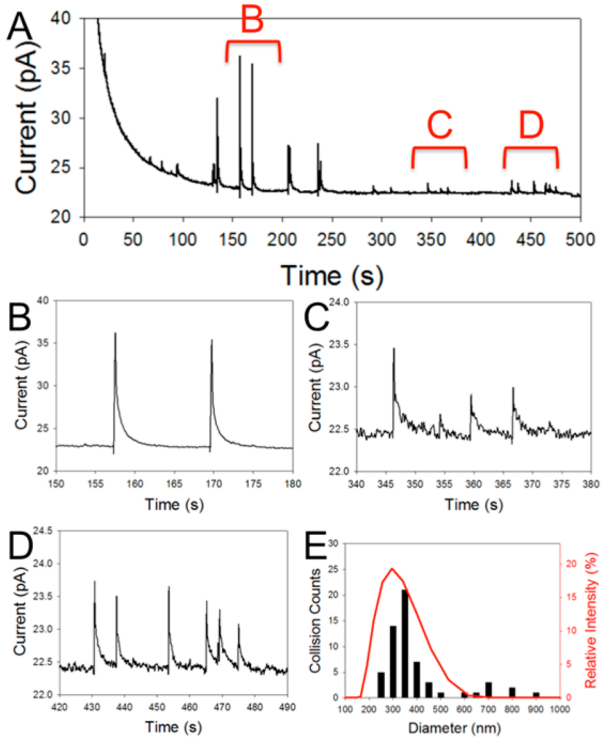

Figure 3. (A) Amperometric *i*−*t* curve of emulsion droplet collisions at C-UME. The measurement solution contains ca. 25.8 pM NB (TCNQ) emulsion droplets and NB saturated water. (B−D) Magnified *i*−*t* curves showing clear spike-shaped responses. The C-UME was biased at −0.45 V vs Ag/AgCl over the entire experimental time. (E) Comparison of droplet size distribution from eq 3 (black bars) vs DLS data (red line).

response was usually observed, which was ascribed to the electrolysis of TCNQ in a single NB emulsion droplet. Peaks in Figure 3A are related to the diffusion and migration of emulsion droplets to the C-UME. The diffusion coefficient of an emulsion droplet (D_{ems}) can be estimated by the Stokes−Einstein equation, eq 1,

$$D_{ems} = \frac{k_B T}{6\pi\eta r_{ems}} \tag{1}$$

where k_B is the Boltzmann constant, T is temperature, η is the viscosity of water (8.94×10^{-4} Pa·s) at 25 °C, and r_{ems} is the radius of an emulsion droplet. From this equation, the diffusion coefficient of a 291 nm diameter emulsion droplet is 1.69×10^{-8} cm^2 s^{-1}. The collision frequency (f_{ems}) governed by the diffusion of the emulsion droplet can be calculated by eq 2,[20]

$$f_{ems} = 4D_{ems}C_{ems}r_{elec}N_A \tag{2}$$

where C_{ems} is the concentration of emulsion droplets, r_{elec} is the radius of the UME, and N_A is Avogadro's number. The predicted frequency of NB (TCNQ) emulsion droplet collisions is 0.53 Hz. Experimentally observed frequency 0.17 Hz is consistent with the theoretically calculated collision frequency within a typical variation associated with stochastic measurements. This result indicates that the collision of droplets on a C-UME is mainly governed by diffusion.

Furthermore, the current in a transient can be integrated to obtain the amount of charge for the reduction of TCNQ in a single emulsion droplet. From the integrated charge, we can estimate the size of the collided NB (TCNQ) droplet. Therefore, we assume that all spherical emulsion droplets (independent of their sizes) contain 20 mM TCNQ, and that all TCNQ in the droplets is completely electrolyzed during a collision event. The droplet diameter (d_{drop}) can be calculated by eq 3,[10]

$$d_{drop} = 2\sqrt[3]{\frac{3Q}{4\pi nFC_{redox}}} \tag{3}$$

where Q is the integrated charge from the spike peak, n is the number of electrons transferred per molecule, F is Faraday's constant, and C_{redox} is the concentration of the redox molecules in a droplet. The droplet size distribution based on eq 3 is presented in Figure 3E. Notably, the size distribution from the electrochemical measurements (black bars in Figure 3E) and that obtained by DLS (red line in Figure 3E) measurement exhibit agreement, implying that our assumption was reasonable for the interpretation of electrochemical results. Moreover, the electrochemical measurement detected some big droplets (650−900 nm), which were not detected by the DLS measurements.

3.1.3. i−t Decay Behavior of TCNQ Peak during the Collision Measurement of NB (TCNQ) Emulsion Droplet. In the previous work with ferrocene in toluene emulsion, we have shown that the electrolysis of redox molecule in a single emulsion droplet showed similar behavior to bulk electrolysis, where the current exponentially decayed with time.[10] Briefly the model assumed is that the colliding droplet attaches while opening a small circular disk electrode, which serves to electrolyze the contents. During the electrolysis, charge neutrality in the droplet must be maintained. Thus, the cation product (ferrocenium) must leave the emulsion droplet, or a counteranion from the aqueous phase should enter. Likewise, we could also explain the new emulsion system for TCNQ reduction electrolysis by a bulk electrolysis model (Figure 4). Equations 4 and 5 express the *i*−*t* behavior of bulk electrolysis,[21]

$$m = \frac{4D_{TCNQ}}{\pi r_e} \tag{4}$$

$$i(t) = i_p\, e^{-(mA/V)t} \tag{5}$$

where m is the mass-transfer coefficient for a disk electrode, D_{TCNQ} is the diffusion coefficient of TCNQ in NB (TCNQ) emulsion droplets, and r_e is the effective contact radius between UME and the emulsion droplet upon the collision. The calculated mass-transfer coefficient is subsequently used as the exponent in eq 5. Here, i_p is the peak current, A is the effective contact area between UME and the emulsion droplet calculated from r_e, V is the emulsion droplet volume, and t is the electrolysis time. In eq 4, D_{TCNQ} and r_e values are experimentally obtainable. D_{TCNQ} is calculated from CV in Figure 2 using eq 6,[21]

DOI: 10.1021/ja512065n
J. Am. Chem. Soc. 2015, 137, 2343−2349

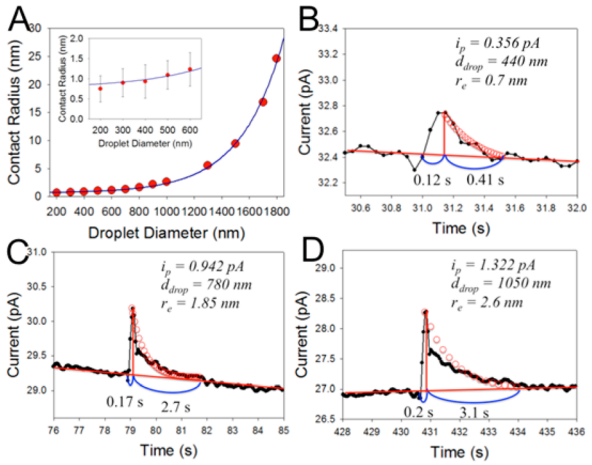

Figure 4. (A) Plot of contact radius (r_e) vs droplet diameter (d_{drop}) of NB (TCNQ) emulsion droplet. The red circles represent the average values of contact radius including standard deviation from experimental data points calculated by eq 7. At least three data points used to calculate the average values and standard deviations in the inset figure. The blue line is the nonlinear regression plot with exponential growth model. (B–D) Enlarged i–t curve and analysis of single current spike. The experimental data were obtained at every 50 ms (black dots). The simulated i–t decay behavior (red circles) was obtained by eq 5. The d_{drop} is calculated from the integrated charge and eq 3.

$$D_{TCNQ} = \frac{i_{ss}}{4nFC_{TCNQ}r_{elec}} \quad (6)$$

where i_{ss} is the steady-state current. C_{TCNQ} is the concentration of TCNQ. The resultant D_{TCNQ} is 6.60×10^{-7} cm^2 s^{-1}. r_e can be calculated from eq 7,[21]

$$r_e = \frac{i(t)}{4nFD_{TCNQ}C^*_{TCNQ}(t)} \quad (7)$$

When a single droplet lands on an UME, within a very short time (0.1–0.2 s), the droplet forms a tiny disk electrode on the UME with an effective contact radius, r_e (Figure 4B–D). After this short landing time, the current exponentially decays with time as TCNQ is consumed by electrolysis. In the initial condition at $t \approx 0$, $C^*_{TCNQ}(t) = C^*_{TCNQ}(0)$, which is 20 mM. Assuming that $i(0) = i_p$ at $t \approx 0$ with $C^*_{TCNQ}(0) \approx 20$ mM, r_e can be estimated for different sized droplets using eq 7. Accordingly, r_e is plotted versus d_{drop} in Figure 4A. Likewise, we obtained a regression plot and corresponding equation by computing the nonlinear regression analysis with exponential model as shown in Figure 4A and eq 8.

$$r_e = 0.75 + 0.058\, e^{0.0033 d_{drop}} \quad (8)$$

The extracted r_e for the different size of emulsion droplets from eq 8 was further used to predict the i–t decay behavior. With the assumption that the droplet volume and contact radius does not change during the electrolysis, the predicted i–t decay (red circles in Figure 4B–D) agrees well with the experimental i–t curves (black lines in Figure 4B–D), implying that the TCNQ reduction in NB (TCNQ) emulsion droplet follows the bulk electrolysis model in the same way as ferrocene oxidation in a toluene emulsion droplet.[10] In this case charge neutrality is maintained by the product ($TCNQ^{\bullet-}$) leaving the droplet into the water phase. In both cases the product ions are sufficiently hydrophilic to be transported readily across the NB/water boundary.

3.2. Single Collision Events of NB Emulsion Droplets.

3.2.1. Electrochemical Reduction of Bulk NB in Various Conditions. In addition to observing TCNQ reduction in the NB emulsion, one can also study the reduction of NB, since it undergoes multiple electron transfers accompanied by proton transfers in aqueous media, as a function of pH and other variables. For example, a four-electron-transfer reaction to produce phenylhydroxylamine (PHA) accompanied by four proton transfers is found in an aqueous solution at pH 5 or 6.[22−24] Thus, we assume a NB emulsion droplet also undergoes a four-electron-transfer reduction during a collision at an UME under constant applied potential. In this case, a single NB emulsion droplet contains ca. 8.15 M NB including 200 mM IL-PP, thus a relatively large reduction current is expected during the electrolysis of the entire NB droplet due to the high concentration of NB as well as four electrons transferred for each NB molecule. Since the reduction potential of NB depends on the pH and medium composition, CVs of NB under various medium conditions were measured prior to the collision experiments with single emulsion droplets. A CV of bulk NB (8.15 M) with 200 mM IL-PP was measured with a C-UME at a scan rate of 30 mV s^{-1}. As shown in Figure 5 (black line), the reduction of NB started around −0.65 V and did not reach a steady state due to the low conductivity of solution and a high concentration of NB, even though the solution had 200 mM IL-PP. A CV of 10 mM NB in water was measured to check the background reaction in the continuous phase. The solubility of NB in water is low (0.19 g NB/100 mL water at 20 °C), but high enough (ca. 15 mM)[25] to give a significant background current. Because the aqueous continuous phase in collision experiments is saturated with NB, the background reaction of NB in water should be understood. As presented in Figure 5 (red line), the reduction of NB in water started around −0.71 V, thus potentials less than −0.71 V is advantageous to avoid high background current for sensitive measurements. A CV was measured in 10 mM NB with 100 mM KCl, 50 mM phosphate buffer (PB) (pH 7) (blue line in Figure 5). In the presence of electrolyte, the reduction of NB started around −0.55 V and reached a steady state around −0.8 V. Overall, the

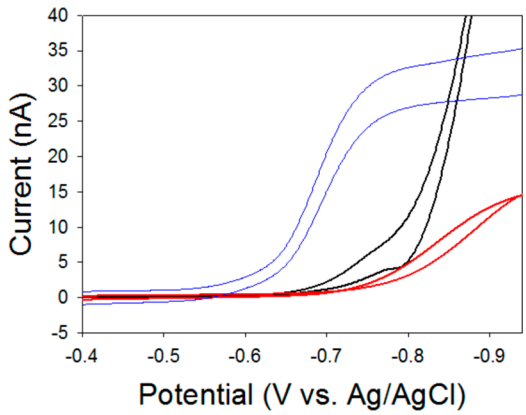

Figure 5. CVs of neat (8.15 M) NB with 200 mM IL-PP (black line), 10 mM NB in water with no electrolyte (red line), and 10 mM NB with 100 mM KCl in 50 mM PB pH 7 (blue line) with C-UME at a scan rate of 30 mV s^{-1}. Even with the small currents, the red trace shows the effects of uncompensated resistance in the electrolyte-free medium.

DOI: 10.1021/ja512065n
J. Am. Chem. Soc. 2015, 137, 2343−2349

results from three CVs in various media suggested that water can serve as a proton source and the electrolyte is important in determining the potential for the reduction of NB, although three CVs do not represent the exact condition for the collision experiments. In fact, the NB emulsion droplet does not contain protons, which exist only in the continuous phase. Contrarily, electrolyte (IL-PP) is only inside of NB emulsion droplets due to its low solubility in water (0.91 mg/100 mL at 20 °C).[26] However, particularly, all the components including NB, electrolyte and proton are present in the reaction zone (at the interface of dispersed and continuous phases), favorable electrolysis of NB in the emulsion droplet may proceed. Therefore, the electrolysis of NB emulsion droplet can occur at less negative potential than −0.71 V, where bulk NB without supporting electrolyte starts to be reduced. Therefore, we applied −0.65 V to sensitively monitor the reduction of NB in a collision experiment. This reduction potential is in a fairly delicate range. Potentials less negative are insufficient to reduce NB, while more negative potentials can increase the background current. In this regard, we believe −0.65 V is the optimum potential to observe the reduction of a NB emulsion sensitively with the low background current.

3.2.2. Collision Experiments of NB Emulsion Droplets at C-UME. Collisions of NB emulsion droplets at a C-UME were measured by amperometric *i*−*t* curve with 22.8 pM NB emulsion droplets at a bias potential of −0.65 V (Figure 6). Many large current spikes were observed during the measurement time. The peak current heights of NB emulsion droplet collisions ranged from 10 to 220 pA, which is almost 20 times higher than that in NB (TCNQ) emulsion droplet collision experiments (0.3−13 pA). These large current spikes result from the high concentration of NB (8.15 M) in NB emulsion droplets. Correspondingly, the electrolysis times for NB emulsion droplet electrolysis (3−15 s) was almost 5 times longer than that with NB (TCNQ) emulsion droplets (0.4−3.1 s). Moreover, we could estimate the collision frequency, f_{ems} = 0.31 Hz. This value is comparable to the predicted collision frequency, 0.60 Hz, calculated by eq 2 with average diameter of NB emulsion, 225 nm from DLS measurement, and subsequently obtained $D_{ems} = 2.18 \times 10^{-8}$ cm^2 s^{-1} from eq 1. The difference between the predicted and experimentally measured f_{ems} is still within the usual variations of measurements of stochastic events, implying that the collisions are mainly governed by the diffusion of the droplets. The d_{drop} was also obtained from the integrated charge and eq 3, and the distribution of the corresponding collision signals shown in Figure 6E. Notably, the overlay of size distribution from the electrochemical measurements and DLS show agreement. Here, the electrochemical data also could detect some big droplets (500−700 nm) which were not detected by the DLS measurements.

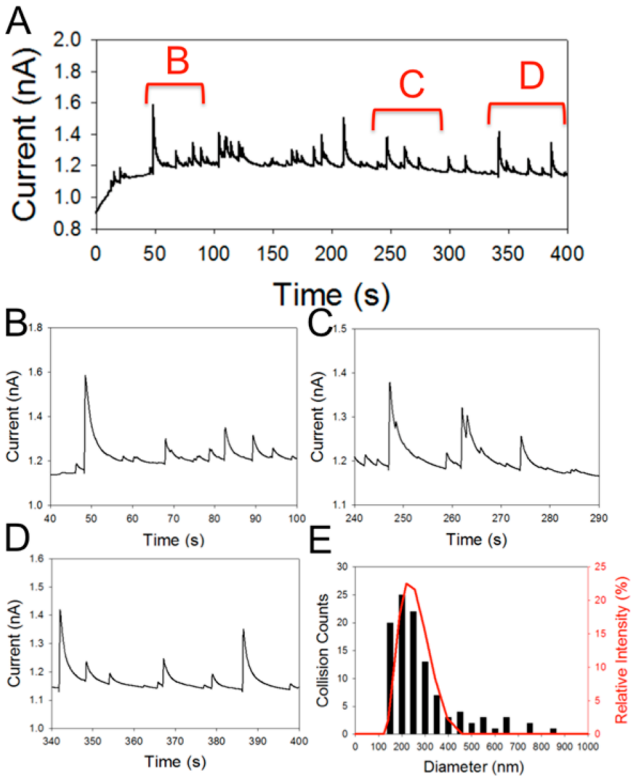

Figure 6. (A) Amperometric *i*−*t* curve of single emulsion droplet collision at C-UME. The solution contains 22.8 pM NB emulsions and NB saturated water. (B−D) Magnified *i*−*t* curves showing clear spike-type responses. The UME potential was −0.65 V vs Ag/AgCl over the entire experimental time. (E) Comparison of droplet size distribution from eq 3 (black bars) vs DLS data (red line).

3.2.3. i−t Decay Behavior of NB Reduction in the NB Emulsion Droplet during the Collision Measurement. The *i*−*t* decay of NB emulsion droplet upon collision shows similar behavior to bulk electrolysis. However, the electrolysis of NB emulsion droplet may not be mass-transport controlled, since the applied potential is not negative enough. Furthermore, the reduction of NB to PHA is affected by the pH of the solution because proton transfer accompanies the electron-transfer reaction of NB. Thus, to account for possible kinetic effects, we modified eq 5 for the *i*−*t* decay behavior by replacing the mass-transfer coefficient (m) in eq 5 by a general kinetic term, k_{eff}, so that the overall current decay with time is described by eq 9,

$$i(t) = i_p\, e^{-(k_{eff}A/V)t} \tag{9}$$

where k_{eff} is an effective kinetic constant of the overall reaction that includes electron-transfer, ion-transfer, and coupled chemical reactions. We defined k_{eff} as a complex term for several factors that influence the electrolysis of a NB emulsion droplet, such as insufficient potential, and proton accessibility to NB. The separation of k_{eff} into each factor and calculating exact values at present cannot be accomplished because of the complexity in the NB reduction reaction of the emulsion droplet. When the NB emulsion droplet collides at an UME, the droplet forms a "tiny disk electrode" with effective radius, r_e. Here, we assume that the NB and NB (TCNQ) emulsion droplets form a disk electrode with a similar, r_e value and the droplet volume does not change during the electrolysis. The fitting of the transient currents in Figure 7 follows eq 9, where we have two adjustable parameters, k_{eff} and A. We calculated A from the r_e, which was referred from experimentally measured value of r_e by collision experiments of NB (TCNQ) (Figure 4A). The current fitting is very sensitive to the change of A value: a small variation in the contact radius can cause a significant change in k_{eff} value by a factor of 4−5. Therefore, it is difficult to extract the exact value of each contact radius of NB droplets on an UME. Here, we display the range of k_{eff} from eq 8, which covers the entire range of contact radii for the corresponding droplet diameter instead of an average value. As

DOI: 10.1021/ja512065n
J. Am. Chem. Soc. 2015, 137, 2343−2349

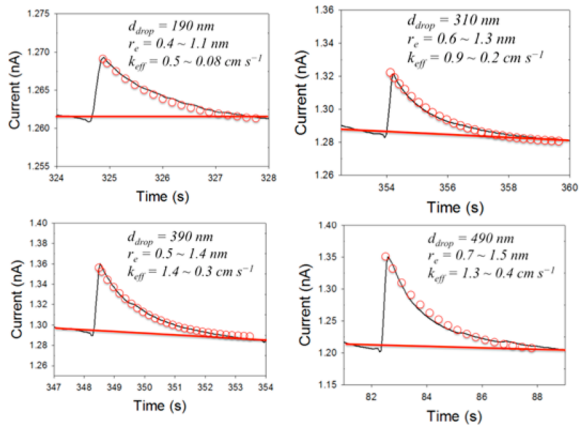

Figure 7. Enlarged $i-t$ curves and analysis of single current spike from NB emulsion droplet electrolysis. The experimental data (black line) agree well with the simulated $i-t$ decay behavior (red circles) calculated from eq 9. The d_{drop} is calculated from the integrated charge and eq 3.

shown in Figure 4A inset, when lower and upper limits of r_e in 300 nm droplet are 0.6 and 1.3 nm, the calculated k_{eff} values are 0.9 and 0.2 cm s^{-1}, respectively. Importantly, the mass transport of NB in the droplet would be highly enhanced up to 2−3 cm s^{-1} due to the nanometer sized contact radius, which can be higher than the calculated k_{eff} by a factor of 3−10. In that sense, we believe that the obtained range of k_{eff} in Figure 7 is reasonable. Overall, we report ranges of r_e and k_{eff} in Figure 7.

3.2.4. Consideration of the Reduction Mechanism of NB Emulsion Droplet and the Fate of the Final Product. The reduction reaction of NB undergoes different pathways depending on the experimental conditions. In a nonaqueous system, NB is reduced to NB$^{\bullet-}$ via a one-electron-transfer reaction,[27] whereas NB is reduced to PHA via four electron transfers accompanied by four proton transfers in an aqueous solution.[22−24] Under the present experimental conditions, NB emulsion droplet provides a nonaqueous environment, while the continuous phase does an aqueous one. Since, the applied potential, −0.65 V is not negative enough to reduce NB to NB$^{\bullet-}$, one-electron-transfer reduction cannot be the dominant pathway even in the emulsion droplet. Rather, at this potential, the reduction of NB to PHA via four-electron transfer with four protons is more plausible in the presence of an aqueous continuous phase. In fact, the droplet sizes estimated from integrated charges assuming four electron transfers are well matched with the DLS results (Figure 6E). Once PHA is formed by the electrochemical reduction in the emulsion droplet, it could take one of the following two paths: remain in the droplet, or leave it and go into the aqueous phase. We can get an idea of the path by the shape of the current response during the collision experiment. If the product, PHA, leaves the emulsion droplet after electrolysis, the volume of emulsion droplet would decrease over the electrolysis time. Accordingly, the concentration of NB in NB emulsion droplet would remain constant over the duration of the electrolysis until NB is completely depleted (Figure 8A). In this case, the stepwise increase in current during the electrolysis would be followed by a sudden decay at completion, thus an overall pulse type current response is expected upon collision. In contrast, if the product, PHA, stays in the emulsion droplet (Figure 8B), the volume of the emulsion droplet would not change, so the concentration of NB in the NB emulsion droplet would exponentially decrease with time during the electrolysis. As a result, we can expect the exponential decay of the $i-t$ curve like bulk electrolysis. In fact, the observed $i-t$ decay of a NB emulsion droplet during collisions followed the latter case, showing good agreement with the predicted $i-t$ behavior from eq 9. In this regard, our speculation about a plausible reduction mechanism and the destiny of the final product appears to be consistent with our experimental results.

4. CONCLUSIONS

We demonstrated a novel strategy to study the electrochemistry of emulsion droplets by monitoring their collisions. First, we showed electrochemical reduction of a redox molecule, TCNQ, in NB emulsion droplets. At an optimum potential, the selective reduction of TCNQ was measured in NB (TCNQ) emulsion droplets. A spike-type current response was observed upon a collisions over the experimental time. We quantitatively analyzed the collision response, collision frequency, and size distribution of the emulsion droplets. Subsequently, the $i-t$ decay behavior was discussed. Second, we further extended our study to the electrochemical reduction of the emulsion droplet itself. For this study, NB emulsion droplets were used, and their collision responses were observed over the experimental time. The results from this collision measurement were quantitatively analyzed in the same manner as for the NB (TCNQ) emulsion case. A plausible mechanism of NB reduction in the emulsion droplet was discussed. Such a mechanistic consideration as well as the quantitative analysis aids in the understanding of the electrochemistry of emulsion droplet systems better, thereby enabling us to extend its possible practical application. For example, single emulsion droplet collision research can be applied to the study of tiny electrochemical reactors, emulsion droplet sensing through extracting off species of interest into

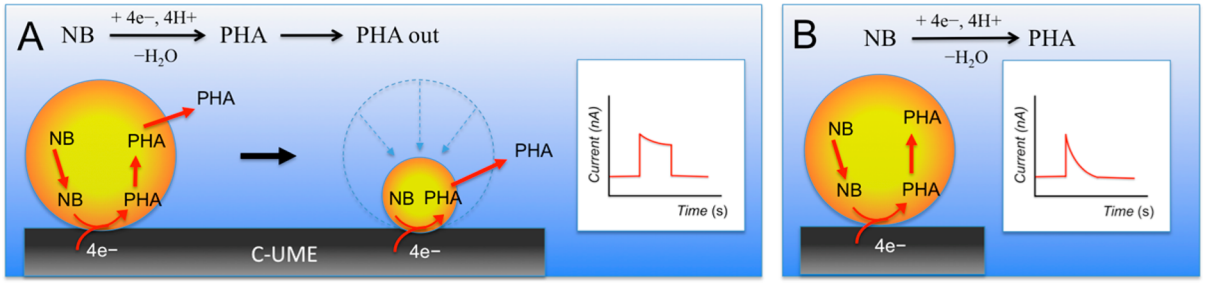

Figure 8. Schematic diagrams of electrolysis of NB emulsion droplet. NB can be reduced to PHA via four electron transfers accompanied by four proton transfers. During electrolysis, (A) the product, PHA, can leave from the emulsion droplet to water, or (B) PHA can stay in the emulsion droplet.

DOI: 10.1021/ja512065n
J. Am. Chem. Soc. 2015, 137, 2343−2349

emulsion droplets, or selective surface modification of electrodes with emulsion droplet collisions.

AUTHOR INFORMATION

Corresponding Author

*ajbard@mail.utexas.edu

Notes

The authors declare no competing financial interest.

ACKNOWLEDGMENTS

This work was financially supported by the National Science Foundation (CHE-1111518) and the Welch Foundation (F-0021).

REFERENCES

(1) Xiao, X.; Fan, F.-R. F.; Zhou, J.; Bard, A. J. *J. Am. Chem. Soc.* **2008**, *130*, 16669−16677.
(2) Kim, J.; Kim, B.-K.; Cho, S. K.; Bard, A. J. *J. Am. Chem. Soc.* **2014**, *136*, 8173−8176.
(3) Zhou, H.; Fan, F.-R. F.; Bard, A. J. *J. Phys. Chem. Lett.* **2010**, *1*, 2671−2674.
(4) Haddou, B.; Rees, N. V.; Compton, R. G. *Phys. Chem. Chem. Phys.* **2012**, *14*, 13612−13617.
(5) Zhou, Y.-G.; Rees, N. V.; Compton, R. G. *ChemPhysChem* **2011**, *12*, 2085−2087.
(6) Kwon, S.; Fan, F.-R. F.; Bard, A. J. *J. Am. Chem. Soc.* **2010**, *132*, 13165−13167.
(7) Fernando, A.; Parajuli, F.; Alpuche-Aviles, M. A. *J. Am. Chem. Soc.* **2013**, *135*, 10894−10897.
(8) Quinn, B. M.; van't Hof, P. G.; Lemay, S. G. *J. Am. Chem. Soc.* **2004**, *126*, 8360−8361.
(9) Boika, A.; Thorgaard, S. N.; Bard, A. J. *J. Phys. Chem. B* **2013**, *117*, 4371−4380.
(10) Kim, B.-K.; Boika, A.; Kim, J.; Dick, J. E.; Bard, A. J. *J. Am. Chem. Soc.* **2014**, *136*, 4849−4852.
(11) Cheng, W.; Compton, R. G. *Angew. Chem., Int. Ed.* **2014**, *53*, 13928−13930.
(12) Omiatek, D. M.; Santillo, M. F.; Heien, M. L.; Ewing, A. G. *Anal. Chem.* **2009**, *81*, 2294−2302.
(13) Omiatek, D. M.; Dong, Y.; Heien, M. L.; Ewing, A. G. *ACS Chem. Neurosci.* **2010**, *1*, 234−245.
(14) Omiatek, D. M.; Bressler, A. J.; Cans, A.-S.; Andrews, A. M.; Heien, M. L.; Ewing, A. G. *Sci. Rep.* **2013**, *3*, No. 1447.
(15) Amatore, C.; Oleinick, A. I.; Svir, I. *ChemPhysChem* **2010**, *11*, 159−174.
(16) Oleinick, A.; Lemaître, F.; Collignon, M. G.; Svir, I.; Amatore, C. *Faraday Discuss.* **2013**, *164*, 33−55.
(17) Scholz, F.; Komorsky-Lovrić, Š.; Lovrić, M. *Electrochem. Commun.* **2000**, *2*, 112−118.
(18) Dick, J. E.; Renault, C.; Kim, B.-K; Bard, A. J. *Angew. Chem., Int. Ed.* **2014**, *53*, 11859−11862.
(19) Dick, J. E.; Renault, C.; Kim, B.-K; Bard, A. J. *J. Am. Chem. Soc.* **2014**, *136*, 13546−13549.
(20) Xiao, X.; Bard, A. J. *J. Am. Chem. Soc.* **2007**, *129*, 9610−9612.
(21) Bard, A. J.; Faulkner, L. R. *Electrochemical Methods, Fundamentals and Applications*, 2nd ed.; John Wiley & Sons: New York, 2001.
(22) Li, Y.-P.; Cao, H.-B.; Liu, C.-M.; Zhang, Y. *J. Hazard. Mater.* **2007**, *148*, 158−163.
(23) Liu, C.; Cao, H.; Li, Y.; Zhang, Y. *J. New Mater. Electrochem. Syst.* **2006**, *9*, 139−144.
(24) Ma, J.; Zhang, Y.; Zhang, X.; Zhu, G.; Liu, B.; Chen, J. *Talanta* **2012**, *88*, 696−700.
(25) Banerjee, S.; Yalkowsky, S. H.; Valvani, C. *Environ. Sci. Technol.* **1980**, *14*, 1227−1229.
(26) Marták, J.; Schlosser, Š. *Sep. Purif. Technol.* **2007**, *57*, 483−494.
(27) Silvester, D.; Wain, A. J.; Aldous, L.; Hardacre, C.; Compton, R. G. *J. Electroanal. Chem.* **2006**, *596*, 131−140.

DOI: 10.1021/ja512065n
J. Am. Chem. Soc. 2015, 137, 2343−2349